

# Paleo-Wildfires and Their Paleoclimatic Effects in Early Permian Coal in the Southern North China Basin

Di Gao, Huiling Guo, Juan Wang,\* Yi Shi, and Di Chen

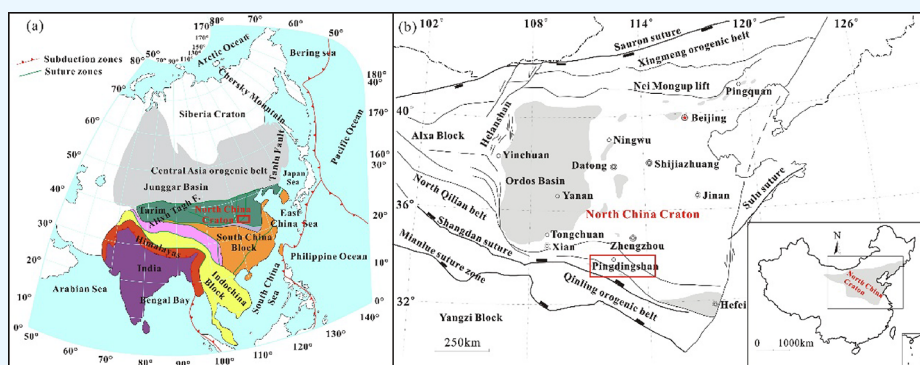
Cite This: *ACS Omega* 2023, 8, 24210–24217

Read Online

ACCESS |

Metrics &amp; More

Article Recommendations



**ABSTRACT:** Paleo-wildfires can help elucidate the transition trends of Earth from “icehouse” to “greenhouse,” thereby allowing us to forecast the current changes associated with wildfires of this era. In this study, the early Permian Shanxi Formation in the Pingdingshan coalfield, located south of the North China Basin, was selected as a study site. Based on data on inertinite content, inertinite reflectance, nine polycyclic aromatic hydrocarbons (PAHs), paleo-wildfires, and their paleoclimate effect during the early Permian coal formation were systematically analyzed. The inertinite content in coal in the study area ranged from 9.76 to 29.65%, with an average of 19.32%. Meanwhile, the average inertinite reflectance values ranged from 2.41–4.74%, with an average of 2.75%. PAHs in the study area were mainly tricyclic and tetracyclic; the contents of fluorene, phenanthrene, pyrene, bypyrene, benzo[*b*]fluoranthene, and benzo[*e*]pyrene were higher than those of other PAHs in the same stratum. The total concentration of PAHs varied widely between layers (3601–21,894 ng/g). The presence of paleo-wildfires was confirmed by the contents of inertinite and PAHs. It can be concluded that paleo-wildfires in the study area were dominated by surface fires at low and medium temperatures based on the combustion equation. The oxygen content in the paleo-atmosphere of the Early Permian Shanxi Formation in the study area was 24.29%, which provided the necessary conditions for the occurrence of wildfires.

## 1. INTRODUCTION

Wildfires not only refer to modern occurrences but also include paleo-wildfire events before the Quaternary period,<sup>1–3</sup> which are an important part of earth systems.<sup>4,5</sup> Paleo-wildfires have been widespread since Silurian plants first emerged on the continent and have had a dramatic impact on terrestrial ecosystems.<sup>2,6–10</sup> Environmental factors and climatic conditions greatly influence the frequency and intensity of wildfires.<sup>4,11</sup> Large-scale wildfire events not only consumed oxygen but also produced large amounts of greenhouse gases and particulate matter, leading to changes in global climate.<sup>6,9,12,13</sup> Therefore, an in-depth study of paleo-wildfires has important significance for exploring the transition trends of the Earth from “icehouse” to “greenhouse” climates.<sup>2,8,11</sup>

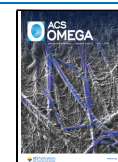
Wildfires warm the atmosphere by emitting black carbon, which is paleoecologically known as charcoal in the  $\mu\text{m}$  and mm sizes,<sup>3,5,8,14</sup> these are also referred to as inertinite in anthracology, with several scholars agreeing that it is the

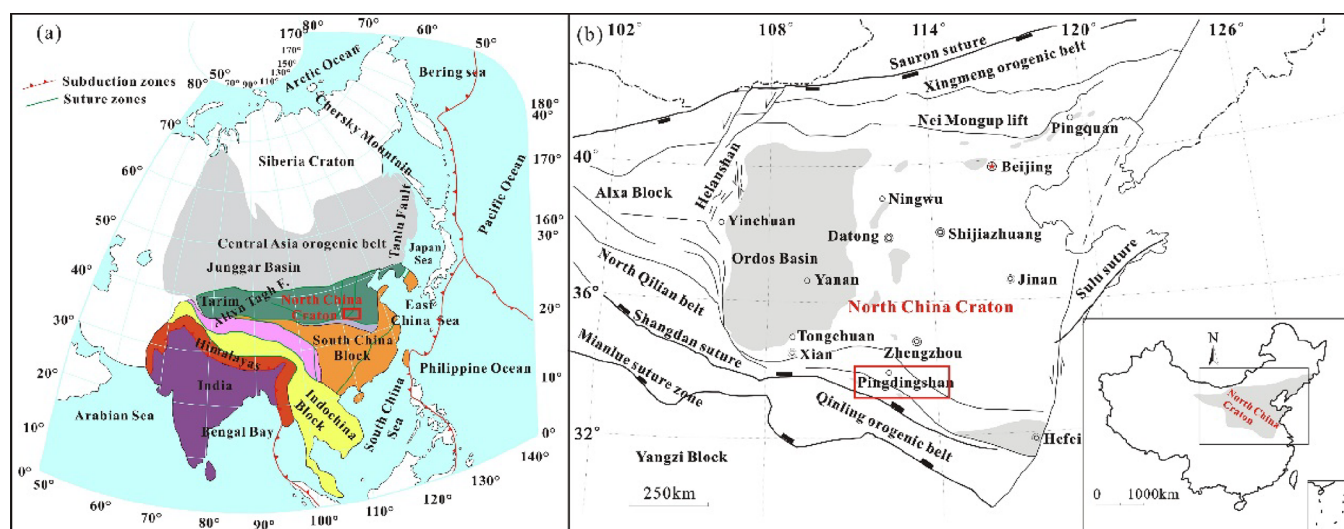
product of the incomplete combustion of plants.<sup>7,14–17</sup> In addition, pyrolytic PAHs are commonly used as evidence of wildfire burning;<sup>18–22</sup> however, most studies on paleo-wildfires have focused on periods of biological mass extinction, such as the Cretaceous–Paleocene,<sup>23,24</sup> Permian–Triassic,<sup>7,25–29</sup> and Jurassic<sup>3,16</sup> extinction events. Meanwhile, the Late Carboniferous–Permian was a globally important period of coal accumulation and a period of major changes in global plate tectonic patterns, climate, marine environments, and ecosystems. Different from previous studies on coal formation in

Received: January 13, 2023

Accepted: June 12, 2023

Published: June 26, 2023





**Figure 1.** Tectonic location map of the study area, (a) Location of the study area in Asia (Modified with permission from ref 17. Copyright Elsevier Ltd., 2012), (b) Location of the study area in the North China Craton (modified with permission from refs 33 and 34. Copyright Royal Society and Elsevier Ltd., 2012).

continental facies, the study area was mainly marine or transitional facies during this period. What is the anomaly in the identification of wildfire events? What is the correlation between the changes of oxygen and carbon content in the atmosphere and the paleoclimate? It is of great significance to the climate environment and carbon cycle that we are facing today, and the study area is located in low latitudes and at the junction of plate tectonics. To address this, this study investigates paleo-wildfire events and their paleoclimatic effects in the Early Permian coals of southern North China. Furthermore, this research provides a scientific basis for the global greenhouse effect by focusing on the identification of macroscopic charcoal in coal rock samples, the content and reflectance of inertinite, and PAH analyses in coal seams.

## 2. GEOLOGICAL BACKGROUND

The Pingdingshan coalfield is situated at the southern margin of the North China Craton and the northern margin of the Qinling orogenic belt (see Figure 1), which is part of the North China Craton Xiaoxiong Tectonic Zone. The regional structural features of NW-trending tensile faults and folds are formed under the influence of the NW-trending tensile stress and tension–torsion stress. Regional structural lines are mostly NW-trending followed by NE-trending, with faults characterized by their large-scale and long extensions.<sup>30–32</sup> The Pingdingshan coalfield is part of the Late Paleozoic coal-bearing basin in North China.

The main coal-bearing strata are the Late Paleozoic Permian coal-bearing rock systems, which are divided from bottom to top into the Lower Permian Taiyuan Formation, Shanxi Formation, Middle Permian Lower Shihezi Formation, and Upper Permian Upper Shihezi Formation, respectively.<sup>31</sup> Since the late Late Carboniferous, the seawater in the study area has undergone large-scale sea regression from the southeast direction, followed by a brief sea immersion, which created a suitable condition for the development of No.2<sub>1</sub>, forming the No.2<sub>1</sub> coal seam with stable deposition and large thickness in the whole area.<sup>35</sup>

## 3. MATERIALS AND METHODOLOGY

Samples of No.2<sub>1</sub> coal were collected from the Early Permian Shanxi Formation of Shoushan Mine, Pingdingshan Coalfield. A total of 13 samples (numbered SY-1 to SY-13, where SY-5 is mudstone gangue) were collected from fresh drill cores at intervals of 20 cm from the bottom to the top and placed into sealed bags immediately after collection.

**3.1. Maceral Identification.** Polished powder coals were prepared according to the GB/T 15590-2008 “Method for Sample Preparation of Coal and Rock Analysis”, and the macerals of coal were identified according to GB/T 8899-2013 “Method for the Determination of Microgroups and Minerals in Coal” by using the oil-soaked lens of a Zeiss Axio Scope A1 microscope with a 10× eyepiece and a 50× objective lens.

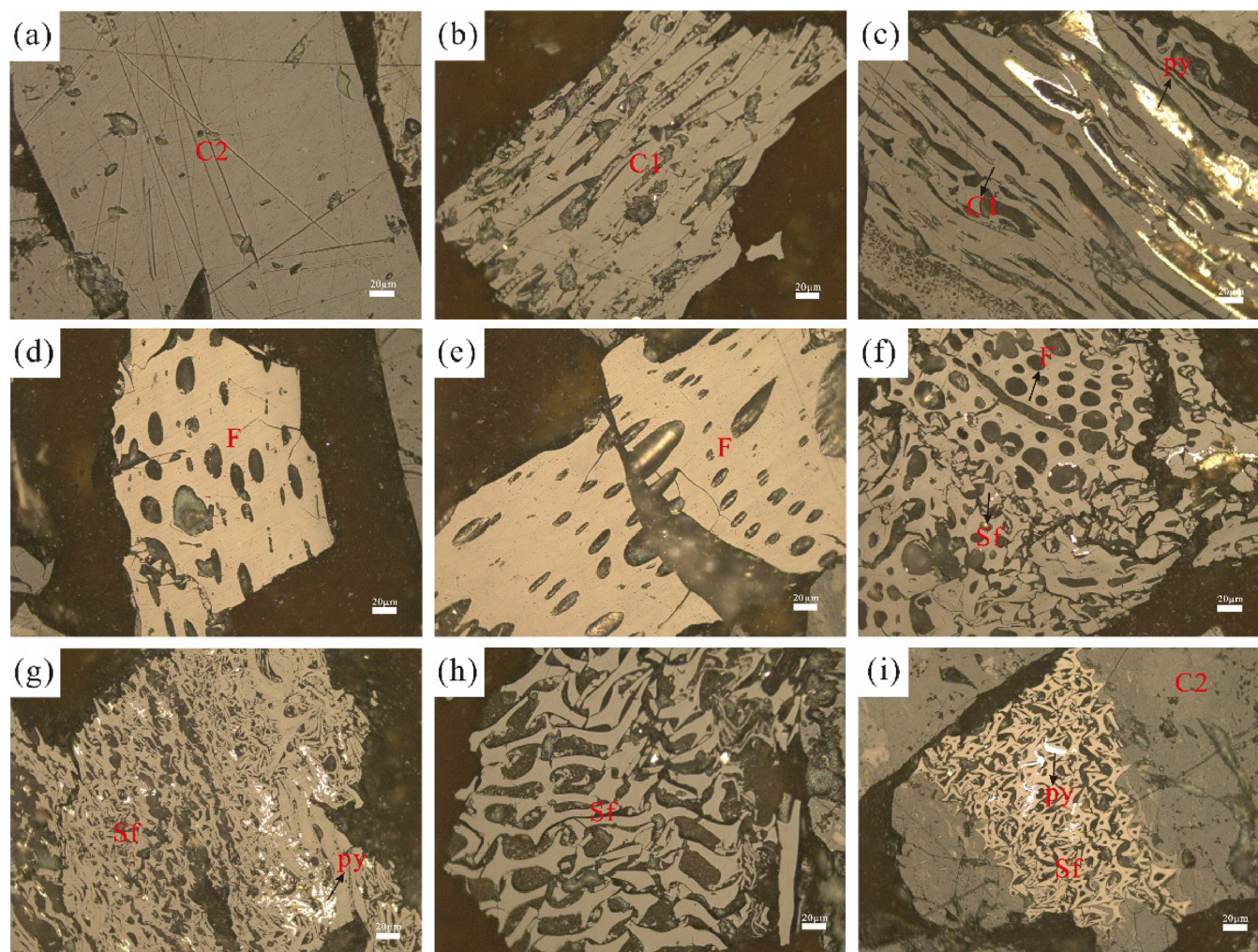
**3.2. Reflectance Determination.** The reflectance of the prepared polished powder coals was determined using a Leica CRAIV 508 DM4P microscope with an eyepiece of 10× and an objective lens of 50× oil immersion, according to GB/T 6948-2008 “Microscopic Determination Method of Reflectance of the Specular Group of Coal”. The aforementioned tests were completed at Henan Polytechnic University in Jiaozuo, China.

**3.3. PAH Testing.** Using an Agilent 6890GC/5975iMS mass spectrometer, the test conditions were as follows: initial temperature of 50 °C was held for 1 min, ramped up to 120 °C at 20 °C per minute, and increased for 25 min at 3 °C/min to 310 °C. The carrier gas used was 99.999% helium with a flow rate of 1 mL/min and an injection temperature of 300 °C. The mass spectrometer was operated in the electron collision mode with an ionization energy of 70 eV and full scan/multi-ion data acquisition, according to the GB/T 18606-2017 standard (“Determination of Biomarkers in Sediments and Crude Oil by Gas Chromatography Mass Spectrometry”). The quality requirements are in line with the national standard GB / T18606-2017, that is, when the blank sample is made, there is no obvious impurity peak in the baseline and the generated mass chromatographic peaks were normally distributed and symmetrical. The precision of the test method the parameter values determined by the comparison experiment obey the normal distribution, and the repeatability and reproducibility are calculated according to the method specified in GB/T 6379.1-



**Table 1. Test Results of the Maceral Content and Reflectance of Vitrinite and Inertinite in Coal Samples**

samples	maceral	minerals	vitrinite	exinite	inertinite	random reflectance of vitrinite	random reflectance of inertinite
SY-1	90.48	9.52	75.49	0	24.51	1.528	2.467
SY-2	88.68	11.32	87.99	1.31	10.70	1.543	2.636
SY-3	87.30	12.70	82.35	2.04	15.61	1.553	2.489
SY-4	87.43	12.57	77.63	1.32	21.05	1.494	2.794
SY-6	50.00	50.00	90.24	0	9.76	1.496	4.740
SY-7	84.16	15.84	84.97	0	15.03	1.491	2.915
SY-8	92.31	7.69	80.41	0	19.59	1.512	2.504
SY-9	90.29	9.71	70.35	0	29.65	1.502	2.548
SY-10	85.80	14.20	82.99	0	17.01	1.509	2.631
SY-11	86.08	13.92	73.77	0	26.23	1.404	2.303
SY-12	89.75	10.25	74.43	0	25.57	1.454	2.539
SY-13	89.33	10.67	82.83	0	17.17	1.443	2.409
average value	85.13	14.87	80.29	0.39	19.32	1.49	2.75



**Figure 2.** Microscopic structural characteristics of maceral: (a–c) desmocollinite (C2) and telocollinite (C1) with pyrite (py); (d, e) fusinite (F) with obvious cell structure; (f) fusinite and semifusinite (Sf); (g–i) semifusinite and pyrite show high reflectivity of pyrite and high relief of semifusinite.

2004. This experiment was performed at the State Key Laboratory of Oil and Gas Resources and Exploration, China University of Petroleum (Beijing).

## 4. RESULTS

**4.1. Macerals in Coal.** The maceral content of coal samples in the study area ranged from 84.16 to 92.31%, with a mean value of 85.13% (see Table 1). The vitrinite group content ranged

from 70.35 to 90.24%, with a mean value of 80.29%; it was dominated by desmocollinite and lenticular telocollinite, followed by telinite and vitrodetrinite and then occasional corpocollinite and gelocollinite (see Figure 2). The inertinite content ranged from 9.76 to 29.65%, with a mean value of 19.32%; it was dominated by semifusinite and fusinite, whose cell structures have been expanded or squeezed and damaged, while also occasionally comprising secretinite and funginite (see

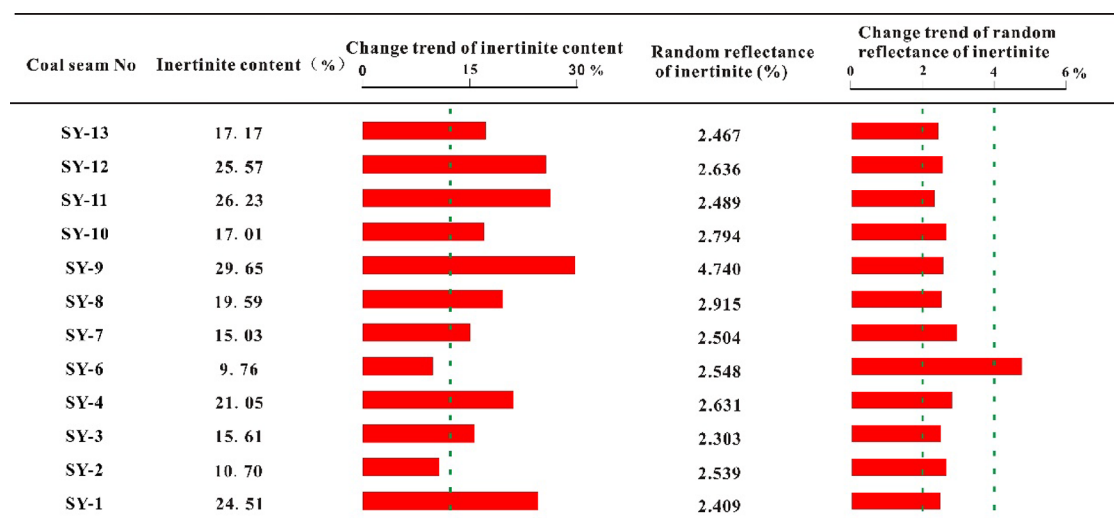


Figure 3. Variation trend of inertinite content and random reflectance test results in coal samples.

Table 2. Contents of PAHs in the Samples

PAHs (ng/g)	SY-1	SY-2	SY-3	SY-4	SY-6	SY-7	SY-8	SY-9	SY-10	SY-11	SY-12	SY-13
Nap.	1	0	0	0	88	1	4	0	0	0	1	14
flu.	3229	2077	695	847	1339	957	1406	762	1467	568	1264	2023
Phe.	12,087	7402	2136	2795	3441	3437	3774	2451	4975	2078	3568	6713
Ant.	18	10	3	4	7	4	6	4	8	3	5	8
FL.	425	239	100	110	115	126	127	80	147	71	133	258
Pyr.	733	392	167	183	194	227	218	138	261	125	231	445
BaA.	213	109	37	52	70	95	82	65	153	70	112	230
CHR.	3097	1438	490	554	527	652	593	371	722	364	696	1252
BbF.	718	331	189	202	125	184	185	112	187	108	246	378
BkF.	70	40	19	22	18	24	21	12	23	13	26	43
Bep.	841	370	345	258	127	208	223	116	185	116	306	459
Bap.	146	66	37	43	35	50	42	24	44	23	47	83
Per.	14	9	1	5	3	4	4	2	3	1	3	6
Bghip.	44	18	18	18	12	19	19	10	16	10	21	31
IP.	166	64	99	73	32	65	72	34	49	34	98	124
DBA.	71	29	17	21	17	28	23	12	23	12	25	39
Cor.	19	7	12	10	5	13	14	7	8	6	19	21
Σ PAHs	21,894	12,602	4364	5195	6155	6096	6811	4201	8270	3601	6801	12,128

Figure 2). The exinite content ranged from 0 to 2.04%, with a mean value of 0.39%. The vitrinite content increased from ~75 to ~90% from SY-1 to SY-6, showing an increasing trend; from SY-6 to SY-13, the content decreased from ~90 to 70%, showing a decreasing trend. The inertinite content decreased from ~24 to ~9% from SY-1 to SY-6, showing a decreasing trend; from SY-6 to SY-13, the content increased from ~9 to ~25%, showing an upward trend (see Figure 3).

**4.2. Reflectance.** The random vitrinite reflectance of coal samples in the study area ranged from 1.404 to 1.553% with a mean value of 1.49%, which is a coking coal of medium–high coal rank metamorphism. The random reflectance of inertinite ranged from 2.409 to 4.740% with a mean value of 2.75%. The reflectance of all samples is ~2.5%, except for sample SY-6, which exhibits a larger value (see Figure 3).

**4.3. Polycyclic Aromatic Hydrocarbons.** A total of 17 PAHs were extracted from coal samples, namely: naphthalene (Nap.), fluorine (Flu.), phenanthrene (Phe.), anthracene (Ant.), fluoranthene (FL.), pyrene (Pyr.), benzo[*a*]anthracene (BaA.), cyclopentane (CHR.), benzo[*b*]fluoranthene (BbF.), benzo[*k*]fluoranthene (BkF.), benzo[*e*]pyrene (Bep.), benzo[*a*]pyrene

(Bap.), Perylene (Per.), benzo[*ghi*]perylene (Bghip.), indeno[1,2,3-*cd*]pyrene (IP.), dibenzo[*a, h*]anthracene (DBA.), and halo benzene (Cor.). In this study, Flu, Phe, Pyr, minerals, BkF, and Bep were at higher levels relative to other PAHs in the same stratum. The total concentration of PAHs also varied in a relatively large range (3601–21,894 ng/g) among different strati, with SY-11 being the lowest and SY-1 the highest (see Table 2). PAHs in the coal samples were classified according to the number of rings, with dicyclic, tricyclic, tetracyclic, pentacyclic, and hexacyclic rings accounting for 0.1, 72.9, 17.6, 8, and 1.3% of the total rings, respectively. Thus, these coal samples were dominated by tricyclic and tetracyclic aromatic hydrocarbons.

## 5. DISCUSSION

### 5.1. Evidence of the Existence of Paleo-Wildfires.

**5.1.1. Charcoal.** Although the genesis of inertinite in coal is still debated in the academic world, with the deepening of research, increasing evidence shows that inertinite is the product of incomplete combustion of plants.<sup>3,5,7,15,16,28,36–38</sup>



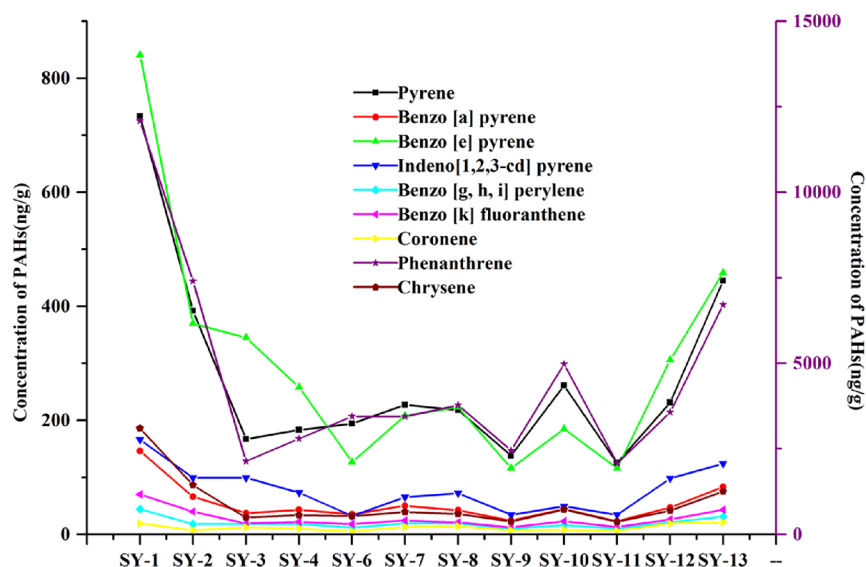


Figure 4. Contents of PAHs in nine combustion sources (PHE and CHR refer to the right ordinate).

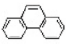
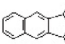

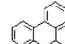
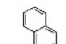
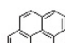
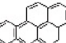
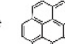
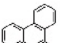
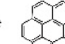
Coal seam No	Total content of 9 PPAHs	Change trend of 9 PPAHs(ng/g)			Change trend of inertinite content		Molecular Formula and Molecular Structure of PAHs			
		0	600	12000	18000	0	15	30 %		
SY-13	17204	[Red bar]			[Blue bar]			phenanthrene C <sub>14</sub> H <sub>10</sub>		Benzo [k] fluoranthene C <sub>20</sub> H <sub>10</sub>
SY-12	9797	[Red bar]			[Blue bar]			pyrene C <sub>16</sub> H <sub>10</sub>		Benzo [g, h, i] perylene C <sub>22</sub> H <sub>12</sub>
SY-11	3322	[Red bar]			[Blue bar]			Chrysene C <sub>18</sub> H <sub>12</sub>		Indeno[1,2,3-cd] pyrene C <sub>22</sub> H <sub>12</sub>
SY-10	3955	[Red bar]			[Blue bar]			Benzo [a] pyrene C <sub>19</sub> H <sub>12</sub>		Coronene C <sub>24</sub> H <sub>12</sub>
SY-9	4392	[Red bar]			[Blue bar]			Benzo [e] pyrene C <sub>20</sub> H <sub>10</sub>		Coronene C <sub>24</sub> H <sub>12</sub>
SY-8	4696	[Red bar]			[Blue bar]					
SY-7	4975	[Red bar]			[Blue bar]					
SY-6	3164	[Red bar]			[Blue bar]					
SY-4	6283	[Red bar]			[Blue bar]					
SY-3	2769	[Red bar]			[Blue bar]					
SY-2	5012	[Red bar]			[Blue bar]					
SY-1	9171	[Red bar]			[Blue bar]					

Figure 5. Variation trends of the total content of PAHs and inertinite from nine combustion sources in coal samples.

Table 3. Parameter Values in Eq 2

	best	max	min
$\sigma_{\min}$ (%)	16	16	16
$\sigma_{\max}$ (%)	35	33	38
$n$	1.8	1.7	1.8

The inertinite content in the study area ranges from 9.76 to 29.65%, with a mean value of 19.32%, which is moderately high compared to that of the Late Carboniferous Taiyuan Formation (<25%), Early Permian Shanxi Formation (20–35%), and Late Permian (<30%) of southern China in the North China Basin,<sup>15,39</sup> and it is moderately low compared to that of the Early and Middle Jurassic of northwest China (30–50%)<sup>39</sup> and the Middle Jurassic (30–50%) in Northwest China.<sup>39</sup> Meanwhile, this is higher than the 4.27% content in peat in the current environment.<sup>40</sup> These values indicate that wildfire events were present in the study area during the Early Permian deposition and occurred significantly more frequently than in the current environment in the region.

**5.1.2. Polycyclic Aromatic Hydrocarbons.** PAHs are commonly used as combustion indicators due to their pyrolytic genesis, especially when they coexist with charcoal.<sup>19,41–43</sup> The most significant source of pyrolytic PAHs is the incomplete combustion of organic matter in forest fires,<sup>43–45</sup> which is considered an indicator of paleo-wildfire events due to its inertness and long-term preservation capacity. The ratio method has been widely applied to determine the source of PAHs. Yunker et al.<sup>45</sup> proposed a method that utilized BaA/228 and IP/(IP + BghiP) ratios to study PAHs sources in the Fraser River basin and concluded that BaA/228 > 0.35 indicates combustion sourcing, BaA/228 < 0.2 indicates petrogenic sourcing, and BaA/228 values between 0.2 and 0.35 are indicative of petroleum combustion. IP/(IP + BghiP) > 0.5 suggests that grass, wood, and coal combustion; IP/(IP + BghiP) < 0.2 indicates petrogenic sourcing and 0.2 < IP/(IP + BghiP) > 0.5 indicates liquid fossil fuel. The BaA/228 ratios in the study area range from 0.16 to 1.01, with the ratios of SY-1, SY-4, SY-6, SY-9, and SY-11 being 0.16, 0.23, 0.31, 0.29, and 0.31, respectively. The remaining seven samples exhibit BaA/228 ratios exceeding 0.35 and IP/(IP + BghiP) ratios greater than 0.5 (0.73–0.85),

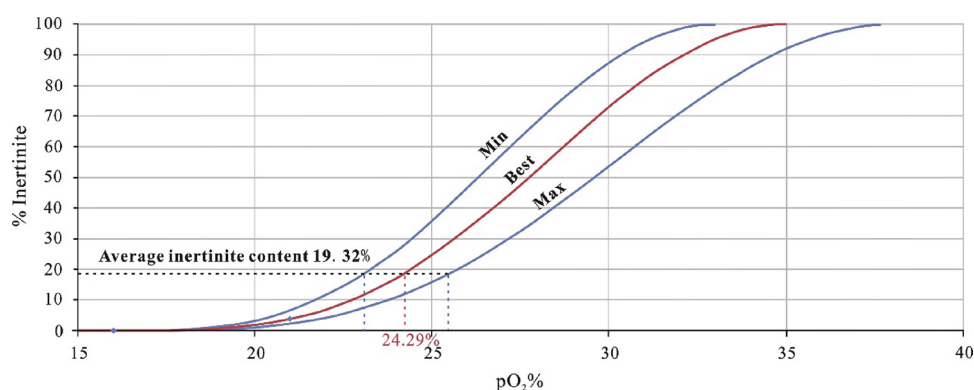


Figure 6. Calibration curve of inertinite content in coal and atmospheric oxygen.

Table 4. Average Content of Inertinite in Shanxi Formation Coal of Early Permian in North China

region	average content of inertinite (%)	reference
Fuxin basin (Liaoning Province)	20.5	15
Xingtai coal field (Hebei Province)	45	15
No. 4 coal in Liulin coal field (Shanxi Province)	14.63	53
No. 5 coal in Liulin coal field (Shanxi Province)	24.62	53
Ordos basin	34.3	54

suggesting that PAHs in coal samples from the study area are mainly derived from biomass combustion and may also have a petroleum source.

According to the classification scheme of Huang et al.,<sup>46</sup> Shen et al.,<sup>42</sup> Song et al.,<sup>43</sup> etc., this paper focuses on the analysis of Phe, Pyr, CHR, BbF, Bep, Bap, Bghip, IP, and Cor, as well as nine pyrolytic PAHs. The change trends of the nine pyrolytic PAHs in the coal of the study area are in good agreement (see Figure 4), and there is a significant increase in the SY-8 and SY-10 seams. The sum of pyrolytic PAHs shows a trend of decreasing and then increasing from bottom to top (see Figure 5), which has a good correlation with the variation trend of inertinite content in coal (see Figure 3), indicating that these nine pyrolytic PAHs are formed via the combustion and thermal decomposition processes during inertinite formation.

**5.2. Types of Paleo-Wildfires.** Based on the spatial distribution of fuels and burning temperatures, paleo-wildfires can be divided into three types: ground, surface, and crown fires.<sup>10,37,47</sup> Ground fire fuels are mainly organic matter such as dead branches and leaves as well as peat from decaying vegetation below the ground surface, and they generally burn at temperatures less than 350 °C. Surface fire fuels include mainly fallen leaves from herbaceous plants, shrubbery, and forest floors, burning at temperatures of ~200–700 °C. Crown fire fuels are mainly produced by fires spreading from the canopy of trees and large shrubs to the canopy and usually burn at temperatures >800 °C.<sup>2,48,49</sup> Scott and Glasspool<sup>38</sup> demonstrated, experimentally, that inertinite reflectance is positively correlated with charcoal formation temperature, and Jones et al.<sup>50</sup> proposed the following combustion equation:

$$T = 184.10 + 117.76 \times R_o\% (r^2 = 0.91) \quad (1)$$

where  $T$  is the temperature at which the charcoal was formed and  $R_o\%$  is the reflectance of the inertinite.

When choosing the value of reflectance, we considered the fact that the microscopic charcoal is light in mass and can be carried to high altitudes by the hot air flow generated during combustion, after which it is carried hundreds or even thousands of kilometers away. Therefore, we needed to choose the average reflectance of the inertinite to estimate the combustion temperature and determine the type of wildfires. The average reflectance of the inertinite in the coal of the study area is ~2.5%, and the burning temperature can be estimated between 455.30 and 742.28 °C according to the formula; this indicates that the type of paleo-wildfire in the early Permian coal-forming period in the study area were mainly surface fires with low and medium temperatures.

**5.3. Early Permian Paleo-Wildfires in Relation to Paleoclimate.** The occurrence of paleo-wildfire requires three factors: fuel, fire source, and oxygen, with oxygen content being a prerequisite that affects flammability. Scott and Glasspool<sup>38</sup> inferred the oxygen content of the paleo-atmosphere based on the charcoal identified in the stratigraphy. Studies have identified 17% oxygen content as the lower limit for natural wildfire occurrence,<sup>38,51</sup> 18.5% for fires to spread, and >23% for wildfires to be frequent.<sup>6,40,52</sup>

Glasspool et al.<sup>40</sup> reconstructed the atmospheric oxygen content over 400 million years based on the relationship between the inertinite content in coal seams and the atmospheric oxygen content; they later refined the model using the following equation:

$$I = \begin{cases} \left( 0.5 - 0.5 \cos \left[ \pi \frac{o - o_{\min}}{o_{\max} - o_{\min}} \right] \right)^n & o_{\min} < o < o_{\max} \\ 0 & o \leq o_{\min} \\ 100\% & o \geq o_{\max} \end{cases} \quad (2)$$

where  $I$  is the inertinite content and  $O$  is the atmospheric oxygen content. Table 3 shows the range of values of  $O_{\min}$ ,  $O_{\max}$ , and  $n$ , where  $O_{\min}$  is the oxygen content when the inertinite content is 0,  $O_{\max}$  is the oxygen content when the inertinite content is 100%, and  $n$  is the maximum gradient of the S curve shown in Figure 6. The average inertinite content in the Early Permian Shanxi Formation coal samples in the study area is 19.32%, and the paleo-oxygen content is 24.29%, as calculated by eq 2, indicating that wildfires were frequent in the study area during this period. Diessel<sup>15</sup> collected the global inertinite content from Devonian to Quaternary coal. The average inertinite content of the Early Permian Shanxi Formation coal in North China is



obtained by adding to the data of the Early Permian Shanxi Formation (see Table 4). The value ranges from 14.63 to 45%, and the average inertinite content in the study area is 19.32%, i.e., within the range in North China, thus indicating that the calculated ancient oxygen content in the study area is reasonable.

## 6. CONCLUSIONS

- (1) The inertinite in the coal of the Early Permian Shanxi Formation in southern North China is dominated by semifusinite and fusinite. Meanwhile, the inertinite content ranges from 9.76 to 29.65% (with an average of 19.32%), which is at a moderately high level compared to the Permian in North China.
- (2) According to the ratio method, PAHs in the coal samples are mainly sourced from biomass combustion and may also be produced via petroleum combustion. The nine pyrolytic polycyclic aromatic hydrocarbons (PAHs) in coal are highly consistent; their content is in accordance with that of inertinite, indicating the existence of paleo-wildfires in the study area. Moreover, the type of wildfire is mainly surface fire at medium and low temperatures.
- (3) The oxygen content of the Early Permian Shanxi Formation paleo-atmosphere in southern North China is inferred to be 24.29% based on the charcoal identified in the stratigraphy, which, when combined with evidence on charcoal and PAHs, suggests the presence of frequent paleo-wildfires in the study area.

## AUTHOR INFORMATION

### Corresponding Author

**Juan Wang** – School of Resources and Environments, Henan Polytechnic University, Jiaozuo 454003, China; Collaborative Innovation Center of Coal Work Safety and Clean High Efficiency Utilization, Jiaozuo 454003, China; Email: 66676872@qq.com

### Authors

**Di Gao** – School of Resources and Environments, Henan Polytechnic University, Jiaozuo 454003, China; State Key Laboratory of Petroleum Resources and Prospecting, China University of Petroleum, Beijing 102249, China; Collaborative Innovation Center of Coal Work Safety and Clean High Efficiency Utilization, Jiaozuo 454003, China; [orcid.org/0000-0001-8541-6563](https://orcid.org/0000-0001-8541-6563)

**Huilin Guo** – School of Resources and Environments, Henan Polytechnic University, Jiaozuo 454003, China

**Yi Shi** – School of Resources and Environments, Henan Polytechnic University, Jiaozuo 454003, China

**Di Chen** – School of Resources and Environments, Henan Polytechnic University, Jiaozuo 454003, China

Complete contact information is available at:

<https://pubs.acs.org/10.1021/acsomega.3c00127>

### Notes

The authors declare no competing financial interest.

## ACKNOWLEDGMENTS

This study is supported by the National Natural Science Foundation of China (no. 41402094), the Foundation of State Key Laboratory of Petroleum Resources and Prospecting, China University of Petroleum, Beijing (no. PRP/open-2008), and the

Fundamental Research Funds for the Universities of Henan Province (no. NSFRF220411).

## ABBREVIATIONS

PAH	polycyclic aromatic hydrocarbon
Flu	fluorene
Phe	phenanthrene
Pyr	pyrene
BaA	benzo[ <i>a</i> ]anthracene
CHR	cyclopentane
BbF	benzo[ <i>b</i> ]fluoranthene
BkF	benzo[ <i>k</i> ]fluoranthene
Bep	benzo[ <i>e</i> ]pyrene
Bap	benzo[ <i>a</i> ]pyrene
Bghip	benzo[ <i>ghi</i> ]perylene
IP	indeno[1,2,3- <i>cd</i> ]pyrene
Cor	indeno[1,2,3- <i>cd</i> ]pyrene.

## REFERENCES

- (1) Glasspool, I. J.; Edwards, D.; Axe, L. Charcoal in the Silurian as evidence for the earliest wildfire. *Geology* **2004**, *32*, 381–383.
- (2) Scott, A. C. The Pre-Quaternary history of fire. *Palaeogeography, Palaeoclimatology, Palaeoecology* **2000**, *164*, 281–329.
- (3) Xu, Y.; Zhang, N.; Zhao, C.; Liang, H.; Sun, Y. Paleo wildfire event in Jurassic coal in Ordos basin and its impact on paleoclimate. *Geol. China* **2022**, *49*, 643–654.
- (4) Bowman, D. M.; Balch, J. K.; Artaxo, P.; Bond, W. J.; Caelson, J. M.; Cochrane, M. A.; et al. Fire in the Earth System. *Science* **2009**, *324*, 481–484.
- (5) Hudspith, V.; Scott, A. C.; Collinson, M. E.; Pronina, N.; Beeley, T. Evaluating the extent to which wildfire history can be interpreted from inertinite distribution in coal pillars: An example from the Late Permian, Kuznetsk Basin, Russia. *Int. J. Coal Geol.* **2012**, *89*, 13–25.
- (6) Belcher, C. M.; Collinson, M. E.; Scott, A. C. *A 450-Million-Year History of Fire*. Oxford: Wiley-Blackwell, 2013, 229–249. DOI: 10.1002/9781118529539.CH12.
- (7) Sun, Y.; Zhao, C.; Püttmann, W.; Qin, S. Evidence of widespread wildfires in a coal seam from the middle Permian of the North China Basin. *Lithosphere* **2017**, *9*, 595–608.
- (8) Scott, A. C.; Fabien, K.; Plotnick, R. E.; Glasspool, I. J.; Chaloner, W. G.; Eble, C. F. Evidence of multiple late Bashkirian to early Moscovian (Pennsylvanian) fire events preserved in contemporaneous cave fills. *Palaeogeogr., Palaeoclimatol., Palaeoecol.* **2010**, *291*, 72–84.
- (9) Scott, A. C.; Chaloner, W. G.; Belcher, C. M.; Roos, C. I. The interaction of fire and mankind: Introduction. *Philos. Trans. R Soc. Lond. B Biol.* **2016**, *371*, 20160149.
- (10) Scott, A. C.; Jones, T. P. The nature and influence of fire in Carboniferous ecosystems. *Palaeogeogr., Palaeoclimatol., Palaeoecol.* **1994**, *106*, 91–112.
- (11) Wang, Y.; Lu, J.; Yang, M.; Yager, J.; Greene, S. E.; Sun, R.; Mu, X.; Bian, X.; Zhang, P.; Shao, L.; Hilton, J. Volcanism and wildfire associated with deep-time deglaciation during the Artinskian (early Permian). *Global Planetary Change* **2023**, *225*, No. 104126.
- (12) Cofer, W. R.; Winstead, E. L.; Stocks, B. J.; Goldammer, J. G.; Cahoon, D. R. Crown fire emissions of CO<sub>2</sub>, CO, H<sub>2</sub>, CH<sub>4</sub>, and TNMHC from a dense Jack pine boreal forest fire. *Geophys. Res. Lett.* **1998**, *25*.
- (13) Flannigan, M. D.; Krawchuk, M. A.; Groot, W. D. J.; Wotton, B. M.; Gowman, L. M. Implications of changing climate for global wildland fire. *Int. J. Wildland Fire* **2009**, *18*, 483–507.
- (14) Ascough, P. L.; Bird, M. I.; Francis, S. M.; Lebl, T. Alkali extraction of archaeological and geological charcoal: evidence for diagenetic degradation and formation of humic acids. *Journal of Archaeological Science* **2011**, *38*, 69–78.
- (15) Diessel, C. F. K. The stratigraphic distribution of inertinite. *Int. J. Coal Geol.* **2010**, *81*, 251–268.

- (16) Yang, B.; Tian, J.; Feng, S.; Yang, J.; Li, Y. Ancient wildfire events recorded in Middle Jurassic coal in the eastern Junggar Basin. *Coal Sci. Technol.* **2020**, *20*, 261–270.
- (17) Yan, D. P.; Qiu, L. Geology of China and adjacent regions: an introduction. *J. Asian Earth Sci.* **2020**, *203*, No. 104533.
- (18) Venkatesan, M. I.; Dahl, J. Organic geochemical evidence for global fires at the Cretaceous/Tertiary boundary. *Nature* **1989**, *338*, 57–60.
- (19) Killops, S. D.; Massoud, M. S. Polycyclic aromatic hydrocarbons of pyrolytic origin in ancient sediments: evidence for Jurassic vegetation fires. *Org. Geochem.* **1992**, *18*, 1–7.
- (20) Marynowski, L.; Zatoń, M.; Simoneit, B. R. T.; Otto, A.; Jędrysek, M. O.; Grelowski, C.; Kurkiewicz, S. Compositions, Sources and Depositional Environments of Organic Matter from the Middle Jurassic Clays of Poland. *Appl. Geochem.* **2007**, *22*, 2456–2485.
- (21) Marynowski, L.; Szeleg, E.; Jędrysek, M. O.; Simoneit, B. R. T. Effects of Weathering on Organic Matter Part II: Fossil Wood Weathering and Implications for Organic Geochemical and Petrographic Studies. *Org. Geochem.* **2011**, *42*, 1076–1088.
- (22) Van de Schootbrugge, B.; Quan, T. M.; Lindström, S.; Püttmann, W.; Heunisch, C.; Pross, J.; et al. Floral changes across the Triassic/Jurassic boundary linked to flood basalt volcanism. *Nat. Geosci.* **2009**, *2*, 589–594.
- (23) Brown, S. A. E.; Scott, A. C.; Glasspool, I. J.; Collinson, M. E. Cretaceous wildfires and their impact on the Earth system[J]. *Cretaceous Res.* **2012**, *36*, 162–190.
- (24) Manfroi, J.; Dutra, T. L.; Gnaedinger, S.; Uhl, D.; Jasper, A. The first report of a Campanian palaeo-wildfire in the West Antarctic Peninsula. *Palaeogeography, Palaeoclimatology, Palaeoecology* **2015**, *418*, 12–18.
- (25) Jasper, A.; Uhl, D.; Guerra-Sommer, M.; Mosbrugger, V. Palaeobotanical evidence of wildfires in the Late Palaeozoic of South America - Early Permian, Rio Bonito Formation, Paraná Basin, Rio Grande do Sul, Brazil[J]. *Journal of South American Earth Sciences* **2008**, *26*, 435–444.
- (26) Kauffmann, M.; Jasper, A.; Uhl, D.; Meneghini, J.; Osterkamp, I. C.; Zvites, G.; et al. Evidence for palaeo-wildfire in the Late Permian palaeotropics - Charcoal from the Motuca Formation in the Parnaíba Basin, Brazil[J]. *Palaeogeogr., Palaeoclimatol., Palaeoecol.* **2016**, *450*, 122–128.
- (27) Cai, Y. *Wildfire events at the Permian Triassic juncture between Xinjiang and South China*. University of Science and Technology of China, 2019.
- (28) Yan, Z. Sedimentological records of late Permian continental strata in eastern Yunnan and their significance for paleoecological evolution. *China Univ. Mining Technol. Beijing* **2019**, DOI: 10.27624/d.cnki.gzkbu.2019.000221.
- (29) Shen, W.; Zhang, H.; Sun, Y.; Lin, Y.; Liang, T.; Yang, Z.; et al. Stratigraphic Records of the Permian Triassic Boundary Fire: Review and Review of Research Progress. *Adv. Earth Sci.* **2012**, *27*, 613–623.
- (30) Yang, Y.; Chu, J.; Li, J.; Zhang, X. Geological conditions and resource potential evaluation of coalbed methane in Pingdingshan coalfield. *Coal Geol. China* **2019**, *31*, 45–49.
- (31) Zhai, Y.; Li, M.; Pan, J.; Wang, Z.; Wang, X.; Mou, P.; et al. Study on coal facies evolution law of Permian coal seams in the south of Pingdingshan Coalfield. *Coal Sci. Technol.* **2020**, *48*, 191–198.
- (32) Guo, D.; Chuai, X.; Zhang, J.; Zhang, H. Evolution law and distribution characteristics of tectonic stress field in Pingdingshan mining area. *Chin. J. Rock Mech. Eng.* **2022**, *006*, 041.
- (33) Cawood, P. A.; Hawkesworth, C. J.; Pisarevsky, S. A.; Dhuime, B.; Capitanio, F. A.; Nebel, O. Geological archive of the onset of plate tectonics. *Philos. Trans. R. Soc., A* **2018**, *376*, 20170405.
- (34) Liu, S.; Su, S.; Zhang, G. Early Mesozoic basin development in North China: Indications of cratonic deformation. *Journal of Asian Earth Sciences* **2013**, *62*, 221–236.
- (35) Lian, Q. Sedimentary characteristics of Permian coal bearing strata in Pingdingshan coalfield. *Sci. Technol. Info* **2012**, *12*, 119.
- (36) Bustin, R. M.; Guo, Y. Abrupt changes (jumps) in reflectance values and chemical compositions of artificial charcoals and inertinite in coals. *Int. J. Coal Geol.* **1999**, *38*, 237–260.
- (37) Scott, A. C. Observations on the nature and origin of fusain. *Int. J. Coal Geol.* **1989**, *12*, 443–475.
- (38) Scott, A. C.; Glasspool, I. J. The diversification of Paleozoic fire systems and fluctuations in atmospheric oxygen concentration. *Proceedings of the National Academy of Sciences* **2006**, *103*, 10861–10865.
- (39) Han, D. *China Coal Petrology*; China University of Mining and Technology Press: Xuzhou, 1996.
- (40) Glasspool, I. J.; Scott, A. C.; David, W.; Natalia, P.; Shao, L. The impact of fire on the Late Paleozoic Earth system. *Front. Plant Sci.* **2015**, *6*, 756.
- (41) Finkelstein, D. B.; Pratt, L. M.; Curtin, T. M.; Brassell, S. C. Wildfires and seasonal aridity recorded in Late Cretaceous strata from south-eastern Arizona, USA. *Sedimentology* **2005**, *52*, 587–599.
- (42) Shen, W.; Sun, Y.; Lin, Y.; Liu, D.; Chai, P. Evidence for wildfire in the Meishan section and implications for Permian - Triassic events. *Geochim. Cosmochim. Acta* **2011**, *75*, 1992–2006.
- (43) Song, Y.; Algeo, T. J.; Wu, W.; Luo, G.; Xie, S. Distribution of pyrolytic PAHs across the Triassic-Jurassic boundary in the Sichuan Basin, southwestern China: Evidence of wildfire outside the Central Atlantic Magmatic Province. *Earth-Scie. Rev.* **2020**, *201*, No. 102970.
- (44) Choi, S. D. Time trends in the levels and patterns of polycyclic aromatic hydrocarbons (PAHs) in pine bark, litter, and soil after a forest fire. *Sci. Total Environ.* **2014**, *470-471*, 1441–1449.
- (45) Yunker, M. B.; Macdonald, R. W.; Vingarzan, R.; Mitchell, R. H.; Goyette, D.; Sylvestre, S. PAHs in the Fraser River basin: a critical appraisal of PAH ratios as indicators of PAH source and composition. *Org. Geochem.* **2002**, *33*, 489–515.
- (46) Huang, X.; Jiao, D.; Lu, L.; Huang, J.; Xie, S. Distribution and Geochemical Implication of Aromatic Hydrocarbons across the Meishan Permian-Triassic Boundary. *J. China Univ. Geosci.* **2006**, *17*, 49–54.
- (47) Pyne, S. J.; Andrews, P. L.; Laven, R. D. *Introduction to Wildland Fire*. New York: J. Wiley & Sons. Science, 1996, 1160978.
- (48) Davis, K. P. *Forest Fire - Control and Us*. New York: Environmental Science, 1959.
- (49) Petersen, H. I.; Lindström, S. Sofie Lindström. Synchronous Wildfire Activity Rise and Mire Deforestation at the Triassic–Jurassic Boundary. *PLoS One* **2012**, *7*, No. e47236.
- (50) Jones, T. P. Fusain in late Jurassic sediments from the Witch Ground Graben, North Sea, UK. *Mededelingen Nederlands Instituut voor Toegepaste Geowetenschappen TNO-National Geological Survey* **1997**, *58*, 93–103.
- (51) Belcher, C. M.; McElwain, J. C. Limits for Combustion in Low O<sub>2</sub> Redefine Paleotatmospheric Predictions for the Mesozoic. *Science* **2008**, *321*, 1197–1200.
- (52) Chaloner, W. G. Fossil charcoal as an indicator of palaeotatmospheric oxygen level. *Journal of the Geological Society* **1989**, *146*, 171–174.
- (53) Li, B. F.; Wen, X. D.; Li, G. D. High resolution sequence stratigraphy analysis of Carboniferous and Permian in North China. *Earth Sci. Front.* **1999**, *S1*, 81–94.
- (54) Xiao, X. M.; Zhao, B. Q.; Thu, Z. L.; Song, Z. G.; Wilkins, R. W. T. Upper Paleozoic petroleum system, Ordos Basin, China. *Marine Petrol. Geol.* **2005**, *22*, 945–963.